3D+time Left Ventricular Strain by Unwrapping Harmonic Phase with Graph Cuts

Ming Li[1], Himanshu Gupta[2], Steven G. Lloyd[2],
Louis J. Dell'Italia[2], and Thomas S. Denney Jr.[1]

[1] Auburn University MRI Research Center, Auburn, Alabama, USA
[2] Division of Cardiovascular Disease, University of Alabama at Birmingham, Birmingham, Alabama, USA

Abstract. In previous work, a three-dimensional left ventricular strain throughout the cardiac cycle was reconstructed using a prolate spheroidal B-spline (PSB) method with displacement measurements obtained from unwrapped tagged MRI (tMRI) harmonic phase images. Manually placed branch cuts were required for each harmonic phase image to resolve phase inconsistencies and to guide the phase unwrapping (mSUP), which is both labor intensive and time consuming and therefore not proper for clinic application. In this paper, we present an automated graph cuts based phase unwrapping method for myocardium displacement measurement (caSUP) which can be used to compute 3D+time cardiac strain. A set of 8 human studies were used to optimize parameters of the energy function and another set of 32 human studies were used to validate the proposed method by comparing resulted strains with those from mSUP and a feature-based (FB) method using the same PSB strain reconstruction. The automated caSUP strains were close to the manual strains and only required 6 minutes after myocardium segmentation versus $\sim$ 2 hours for the manual method.

1 Introduction

Tagged MRI (tMRI) is an established method for measuring parameters of left ventricular (LV) deformation and strain. Tagged MRI spatially modulates the longitudinal magnetization of the underlying tissue before image acquisition. The result is a periodic tag pattern that deforms with the tissue. Before strain can be estimated, myocardial deformation must be measured. Several techniques have been developed to either manually or automatically measure myocardium deformation from the deformed tag pattern, including feature-based methods [1,2,3], non-rigid registration-based [4,5] methods, and HARmonic Phase (HARP)-based methods [6,7].

Among these techniques harmonic phase (HARP) is the most popular, due to its nature of time efficiency and automation. In HARP analysis, the tag pattern deformation is measured by the local change in the tag pattern phase. The HARP phase at a point in the image is a material property of the underlying tissue and can be tracked through the image sequence or used to compute 2D strain [7]. The

P. Golland et al. (Eds.): MICCAI 2014, Part II, LNCS 8674, pp. 578–585, 2014.

HARP technique, however, has some limitations. First, it cannot compensate for through-plane motion, which limits its application to the condition of 3D analysis. Second, HARP tracking [7] can compute Lagrangian strain but assumes deformation between frames to be less than one-half tag spacing, while HARP strain [6] is Eulerian strain and has no such assumption.

In [8], an unwrapped harmonic phase technique was developed to solve above problems. We refer to this method as manual Strain from Unwrapped Phase (mSUP). Compared to feature-based methods, displacement measurements from mSUP are denser than those obtained from tracking tag lines or tag grid intersections, and are less spatially smoothed than non-rigid registration-based methods. Furthermore, because the phase is unwrapped, it does not assume small motion like HARP tracking does. In [8], a prolate spheroidal B-spline (PSB) method [9] was used to compute left ventricular strain from displacement measurements. The resulted strain is three-dimensional and Lagrangian. However, as discussed in [8], manually placed branch cuts were used to resolve phase inconsistencies, which were referred as residues. In order to get an accurate unwrapped phase image one needs to lay down branch cuts carefully, which requires proficiency and is labor intensive and time consuming.

In this paper, we address this problem by introducing an automated phase unwrapping technique based on integer optimization with graph cuts. As mentioned in [10], the unwrapped phase differs from the wrapped phase at each pixel by an integer multiple of 2π, where the integer is termed as the *wrap count*. Assuming the unwrapped phase is spatially smooth, [10] addressed phase unwrapping problem by implementing a smoothness prior to a first-order Markov random field and optimizing the wrap count at each pixel with dynamic programming. In[11], a similar first-order Markov random field was considered and the wrap count was iteratively optimized with a graph cut technique, referred as phase unwrapping max-flow/min-cut (PUMA). In this paper, we extended the PUMA algorithm by introducing a unary term in the energy function which penalizes the phase difference between two consecutive time frames at each pixel, thus making the unwrapped phase images temporally smooth. Though in [11] the integer field optimized was restricted as non-negative, the integer field in our method can contain negative values.

2 Methods

Phase unwrapping procedure is to reconstruct *absolute phase*, ϕ, from *wrapped phase*, ψ, by adding an integer, k, multiple of 2π, called the *wrap count*.

In [10] and in [11], the ill-posed problem was solved by introducing a smoothness prior probability with first-order neighborhood system to a Markov random field. Then, the unwrapping process is equivalent to the optimization of wrap count image $\mathbf{k}$. [10] used dynamic programming for integer optimization. In [11], the problem was solved efficiently by introducing graph cuts technique. Let $\mathbf{k}^{i+1} = \mathbf{k}^i + \boldsymbol{\delta}$ be the wrap count image at iteration $i+1$ and $\boldsymbol{\delta}$ be a binary image. [11] stated that the integer optimization was equivalent to a sequence of

binary optimizations of $\boldsymbol{\delta}$ until stopping criteria was met (when there was no energy change). The binary optimization at each iteration was efficiently solved by computing max-flow/min-cut of the corresponding graph.

Even though PUMA was successfully applied to certain phase unwrapping problems, its performance in the application of cardiac strain measurement is limited. The reasons are twofold. First, the clique potential energy is nonconvex in order to allow for phase discontinuities between different material regions. A HARP image computed from tMRI may contain many discontinuities due to the presence of different tissue types and air. This poses a nonsubmodular energy optimization problem, which is typically an NP-hard problem, and therefore could not be efficiently solved by max-flow/min-cut method. [11] solved this problem by truncating nonsubmodular terms, rendering the unwrapped phase to be an estimated result. Second, the PUMA method unwraps the phase by finding integers to make the pairwise energy lower, but this may not result in the best unwrapping for myocardial deformation.

In this paper we addressed the first problem by masking out the myocardium region and restricting the integer optimization process only to that region. By doing so, the processing time could be greatly cut because fewer pixels are counted and fewer steps of optimization are required. And, since the masked myocardium region should have no material discontinuities, the phase of this region should be spatially smooth, and we can use a convex clique potential energy with no need of truncating nonsubmodular terms.

For the second problem, we introduced a unary temporal smoothness penalty term to the energy function in [11], the new energy function is

$$\begin{aligned} E(\mathbf{k}^t|\boldsymbol{\psi}^t, \boldsymbol{\phi}^{t-1}) = & \sum_{\{i,j\}|\{i,j\},\{i,j-1\}\in\boldsymbol{\Omega}^t} |2\pi(k^t_{i,j} - k^t_{i,j-1}) + \psi^t_{i,j} - \psi^t_{i,j-1}|^2 \\ & + \sum_{\{i,j\}|\{i,j\},\{i-1,j\}\in\boldsymbol{\Omega}^t} |2\pi(k^t_{i,j} - k^t_{i-1,j}) + \psi^t_{i,j} - \psi^t_{i-1,j}|^2 \\ & + \alpha \sum_{\{i,j\}\in\boldsymbol{\Omega}^t\cap\boldsymbol{\Omega}^{t-1}} |2\pi k^t_{i,j} + \psi^t_{i,j} - \phi^{t-1}_{i,j}|^2, \end{aligned} \tag{1}$$

where $\boldsymbol{\Omega}^t$ and $\boldsymbol{\Omega}^{t-1}$ are masked out regions of interest (ROI) of images at time t and $t-1$, $\mathbf{k}^t$ is the wrap count image of time t, $\psi^t_{i,j}$ and $\phi^{t-1}_{i,j}$ are wrapped phase of time t and unwrapped phase of time $t-1$ at pixel $\{i,j\}$. α is the weight of the unary term. The optimal choice of α will be discussed in Experiments section.

The energy function above uses temporal smoothness to regulate phase unwrapping. We also devised a new framework of steps of binary optimization, because the wrap count could potentially be negative, rather than the situation in [11] where only the pairwise wrap count difference was of importance and the wrap count field could be restricted to be non-negative. The new optimization process could be explained by the *fusion move* described in [12]. Each iteration is composed of two optimizations: a $(0, 1)$ binary optimization and a $(0, -1)$ binary optimization. According to [13], after a series of binary optimization the resulting unwrapped phase is guaranteed to be one of the global solutions.

We could unwrap the HARP image directly using Equation 1, but, instead, we unwrap the demodulated HARP. We do this because the unwrapping of demodulated HARP requires much fewer steps of optimization, which considerably cuts down the processing time. The definition of demodulated HARP is given as

$$\boldsymbol{\psi}' = \mathcal{W}(\boldsymbol{\psi} - \mathcal{W}(\mathbf{u})), \tag{2}$$

where $\boldsymbol{\psi}'$ denotes the demodulated HARP image, $\mathbf{u}$ is the undeformed phase image with no wrapping, $\mathcal{W}(\cdot)$ is the wrapping function. We got the unwrapped demodulated phase $\boldsymbol{\phi}'$ by substituting $\boldsymbol{\psi}'$ for $\boldsymbol{\psi}$ in Equation 1. Finally the unwrapped phase $\boldsymbol{\phi}$ was computed by adding the undeformed phase $\mathbf{u}$ to $\boldsymbol{\phi}'$.

After all the HARP images were unwrapped, we used the PSB method [9] for LV strain reconstruction. We refer to this as computer-assisted Strain from Unwrapped Phase (caSUP).

3 Experiments

All participants underwent MRI on a 1.5T MRI scanner (GE, Milwaukee, WI) optimized for cardiac application. tMRI composed of 8-12 slices of short-axis view and 2 slices for 4 chamber and 2 chamber long-axis view were acquired with a prospectively ECG gated fast gradient-echo cine sequence with grid tags spaced 7mm apart. Scanning parameters were: FOV=40×40cm, scan matrix=256×128, 8mm slice thickness, flip angle=10°, TE=4.2ms, TR=8.0ms, 20 frames per cardiac cycle, typical temporal resolution is 50ms.

All routines were implemented in MATLAB (The Mathworks Inc, Natick, MA). The binary optimization algorithm was in C++ and we made a mex file in order to use it under MATLAB environment. Before phase unwrapping and strain computation, we drew contours on two time frames in each slice and automatically propagated the contours to all other time frames with algorithm in [14]. A typical processing time (not including myocardial contouring) for a whole study (200-280 images) composed of both short-axis and long-axis images is ~ 6 minutes, for automatic phase unwrapping and strain reconstruction.

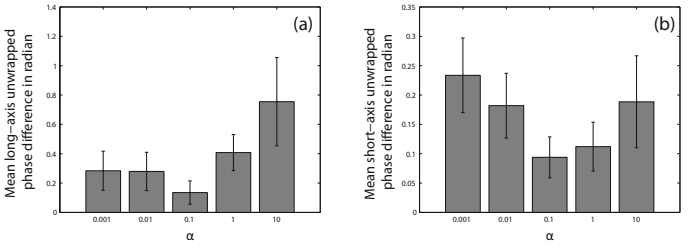

Fig. 1. Mean end-systolic unwrapped differences compared to manual unwrapped phase for different values of α for long-axis slices (a) and short-axis slices (b). Error bars are standard errors.

Table 1. Statistics of differences between strains and torsions from caSUP and mSUP, or caSUP and FB methods for 32 validation studies at ES. Differences = Mean ± Standard Error. ρ = Correlation Coefficient. For all correlation coefficients, $p < 0.001$. CV = Coefficient of Variance. E_{rr} = LV radial strain. E_{cc} = LV circumferential strain. E_{ll} = LV longitudinal strain. E_{min} = LV minimum principle strain.

	caSUP - mSUP				caSUP - FB			
Strain	Differences	p	ρ	CV	Differences	p	ρ	CV
E_{rr} (unitless)	0.0025 ± 0.0063	0.92	0.93	5.50%	-0.0017 ± 0.0072	0.94	0.91	6.19%
E_{cc} (unitless)	0.0000 ± 0.0008	0.99	0.99	0.83%	0.0028 ± 0.0012	0.71	0.98	1.25%
E_{ll} (unitless)	0.0044 ± 0.0027	0.62	0.91	3.79%	0.0030 ± 0.0021	0.73	0.95	2.91%
E_{min} (unitless)	0.0017 ± 0.0013	0.82	0.97	0.99%	0.0041 ± 0.0020	0.57	0.92	1.56%
$Torsion$ (degrees)	0.8112 ± 0.3115	0.23	0.78	4.66%	-0.4241 ± 0.1853	0.54	0.93	2.60%

Table 2. Comparison of strains and torsions computed using caSUP and mSUP. Differences = Mean ± Standard Error. ρ = Correlation Coefficient. CV = Coefficient of Variance. E_{cc} = LV circumferential strain. E_{min} = LV minimum principle strain.

	Strain	Differences	p	ρ	p	CV
E_{cc}	Peak Strain (unitless)	0.0014 ± 0.0001	0.86	0.99	<0.001	0.80%
	Systolic Rate (1/sec)	0.0111 ± 0.0016	0.74	0.93	<0.001	1.70%
	Early-Diastolic Rate (1/sec)	-0.0663 ± 0.0051	0.32	0.81	<0.001	5.25%
E_{min}	Peak Strain (unitless)	0.0230 ± 0.0012	0.06	0.77	<0.001	4.51%
	Systolic Rate (1/sec)	0.0195 ± 0.0030	0.74	0.92	<0.001	2.80%
	Early-Diastolic Rate (1/sec)	0.0037 ± 0.0082	0.96	0.61	<0.001	9.88%
$Torsion$	Peak Strain (degrees)	-0.5718 ± 0.1718	0.77	0.77	<0.001	5.97%
	Systolic Rate (degrees/sec)	1.8959 ± 1.0174	0.86	0.70	<0.001	7.95%
	Early-Diastolic Rate (degrees/sec)	33.4056 ± 2.8551	0.03	-0.11	0.560	19.62%

In order to optimize α in Equation 1, we tested different values on a set of 8 human subjects (2 normal volunteers (NL), 2 hypertensive patients (HTN), 2 diabetic patients with myocardial infarction (DMI), and 2 patients with mitral regurgitation (MR)).We compared the value of $\alpha \in \{0.001, 0.01, 0.1, 1, 10\}$. Each of the values was used for processing the 8 studies and unwrapped phase images at end-systole (ES) were compared to those with manually placed branch cuts (mSUP). Mean unwrapping differences with different α for both long-axis and short-axis images were shown in Figure 1. We chose $\alpha = 0.1$ for the validation experiment.

3.1 Validation

The proposed caSUP method was validated on a cohort of 32 human subjects not used for parameter optimization (8 normal volunteers (NL), 8 hypertensive patients (HTN), 8 diabetic patients with myocardial infarction (DMI), and 8 patients with mitral regurgitation (MR)) with no manual correction to the unwrapped phase. In each subject, 3D left ventricular strains in all timeframes were obtained with caSUP and mSUP methods. Both of these two methods utilize

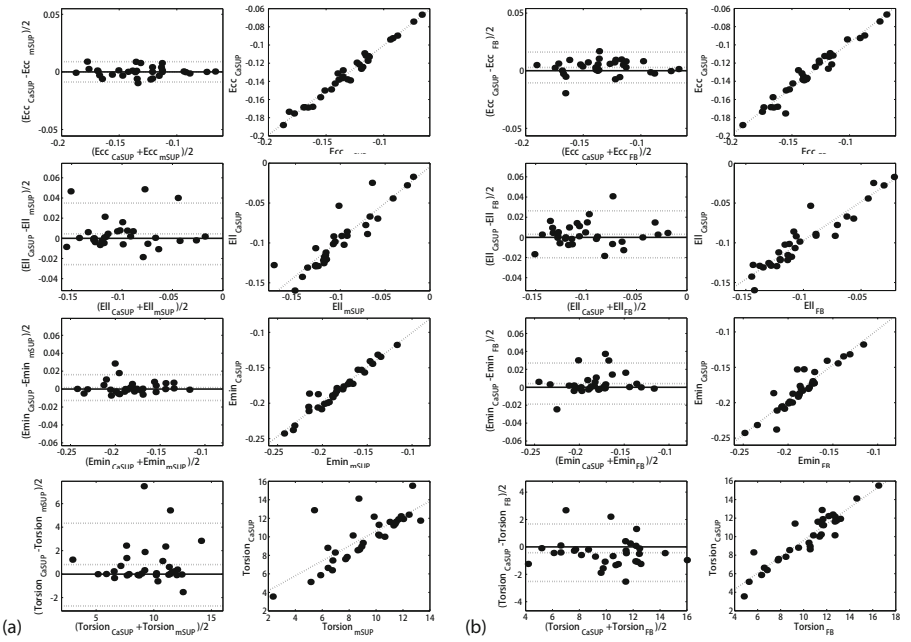

Fig. 2. Bland-Altman (left column) and correlation (right column) plots for comparing caSUP and mSUP (a), caSUP and FB (b) strain measurements at ES time frame. Top to bottom are E_{cc}, E_{ll}, E_{min} (all unitless) and $Torsion$ (in degrees).

the prolate spheroidal B-spline method in [9] to reconstruct strains. Another feature-based (FB) strain as described in [9] was also generated at end-systole.

Table 1 shows the statistics of the difference in averaged mid-ventricular strains and global torsion over the 32 studies between caSUP and mSUP, caSUP and FB methods. For comparison of caSUP and mSUP methods, the caSUP strains and torsion are highly correlated to mSUP strains. CV for E_{cc} and E_{min} are quite low (less than 1%). CV for E_{rr}, E_{ll} and torsion are a bit higher but still reasonable. All the strains and torsion from caSUP method are statistically indifferent from the strains and torsion from mSUP method. For comparison of caSUP and FB methods, strains and torsions are highly correlated too. E_{ll} and torsion have higher correlations with FB than with mSUP. CV for E_{ll} and torsion are also lower, though CV for E_{rr} is a bit higher. All the strains and torsion from caSUP method are statistically indifferent compared to strains and torsion from feature-based method. Comparison between caSUP and mSUP and comparison between caSUP and FB are displayed in Bland-Altman and correlation plots shown in Figure 2(a) and Figure 2(b), respectively.

Figure 3 shows representative maps of 3D minimum principle strains (E_{min}) and rotations at ES computed from FB, mSUP and caSUP methods. Note that the same strain reconstruction method was used (PSB). The strain maps from the three methods are very similar to each other.

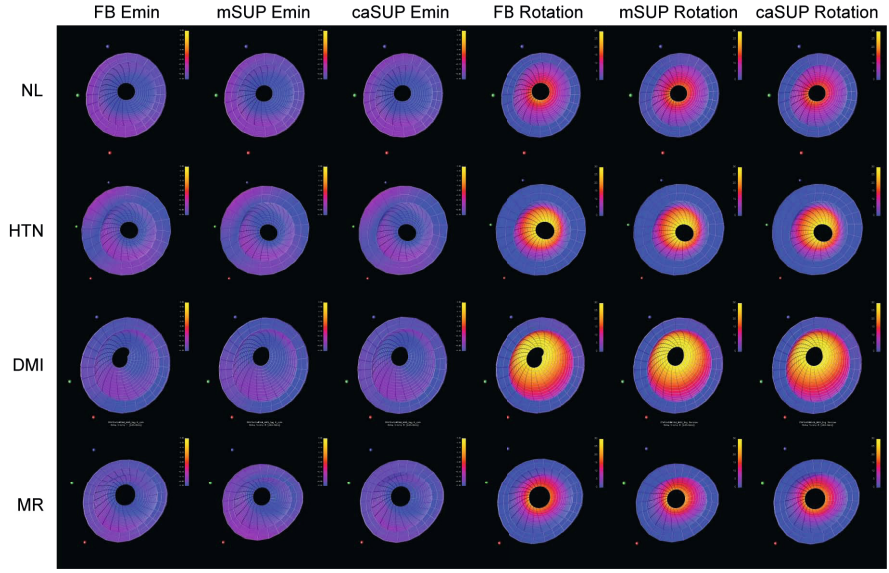

Fig. 3. Maps of minimum principle (E_{min}) strain and rotation at ES using FB, mSUP and caSUP methods for hearts from a normal (NL) volunteer, and patients with hypertension (HTN), diabetes with myocardial infarction (DMI) and mitral regurgitation (MR). E_{min} on the left three columns are mapped from blue = -25% to yellow = 25%. Rotations on the right three columns are mapped from blue = 0° to yellow = 30°.

Table 2 shows statistics of the difference between the 3D+time strains and torsions calculated from caSUP and mSUP methods. We can see the strains and torsion from caSUP are very close to the strains and torsion from mSUP, except for the early-diastolic rate for torsion. The increased differences in early-diastolic rates were partly due to the tag line CNR decrease through the cycle due to T1 decay of the tag pattern.

4 Conclusion

In this paper we proposed an automated phase unwrapping technique with graph cuts for myocardium displacement measurement from tMRI images, which was later on applied to a prolate spheroidal B-spline method for cardiac strain reconstruction. The processing time of phase unwrapping and strain reconstruction for a typical human study (200-280 images) composed of long-axis and short-axis images was ~ 6 minutes. This is a great advantage compared to the mSUP method which requires manual intervention to place branch cuts for each HARP image. The resulted strain is three-dimensional Lagrangian strain. We validated the proposed method on a cohort of 32 human studies and find no significant difference with mSUP and FB methods, suggesting that the proposed method can accurately reconstruct 3D+time strains with considerably less processing time and less user intervention than previous methods.

References

1. Denney, T.S., McVeigh, E.R.: Model-free reconstruction of three-dimensional myocardial strain from planar tagged MR images. J. Magn. Reson. Imaging 7(5), 799–810 (1997)
2. Guttman, M.A., Prince, J.L., McVeigh, E.R.: Tag and contour detection in tagged MR images of the left ventricle. IEEE Transactions on Medical Imaging 13(1), 74–88 (1994)
3. Qian, Z., Montillo, A., Metaxas, D.N., Axel, L.: Segmenting cardiac MRI tagging lines using Gabor filter banks. In: Proceedings of the 25th Annual International Conference of the IEEE ngineering in Medicine and Biology Society, vol. 1, pp. 630–633. IEEE (2003)
4. Chandrashekara, R., Mohiaddin, R.H., Rueckert, D.: Analysis of 3-D myocardial motion in tagged MR images using nonrigid image registration. IEEE Transactions on Medical Imaging 23(10), 1245–1250 (2004)
5. Ledesma-Carbayo, M.J., Derbyshire, J.A., Sampath, S., Santos, A., Desco, M., McVeigh, E.R.: Unsupervised estimation of myocardial displacement from tagged MR sequences using nonrigid registration. Magn. Reson. Med. 59(1), 181–189 (2008)
6. Osman, N.F., McVeigh, E.R., Prince, J.L.: Imaging heart motion using harmonic phase MRI. IEEE Transactions on Medical Imaging 19(3), 186–202 (2000)
7. Osman, N.F., Kerwin, W.S., McVeigh, E.R., Prince, J.L.: Cardiac motion tracking using CINE harmonic phase (HARP) magnetic resonance imaging. Magn. Reson. Med. 42(6), 1048–1060 (1999)
8. Venkatesh, B.A., Gupta, H., Lloyd, S.G., Dell'Italia, L., Denney, T.S.: 3D left ventricular strain from unwrapped harmonic phase measurements. J. Magn. Reson. Imaging 31(4), 854–862 (2010)
9. Li, J., Denney, T.S.: Left ventricular motion reconstruction with a prolate spheroidal B-spline model. Phys. Med. Biol. 51(3), 517–537 (2006)
10. Ying, L., Liang, Z.P., Munson, D.C., Koetter, R., Frey, B.J.: Unwrapping of MR phase images using a Markov random field model. IEEE Transactions on Medical Imaging 25(1), 128–136 (2006)
11. Bioucas-Dias, J.M., Valadao, G.: Phase unwrapping via graph cuts. IEEE Transactions on Image Processing 16(3), 698–709 (2007)
12. Lempitsky, V., Rother, C., Roth, S., Blake, A.: Fusion moves for markov random field optimization. IEEE Transactions on Pattern Analysis and Machine Intelligence 32(8), 1392–1405 (2010)
13. Kolmogorov, V.: Primal-dual algorithm for convex Markov random fields. Microsoft Research MSR-TR-2005-117 (2005)
14. Feng, W., Nagaraj, H., Gupta, H., Lloyd, S.G., Aban, I., Perry, G., Calhoun, D., Dell'Italia, L., Denney, T.S.: A Dual Propagation Contours Technique for Semi-Automated Assessment of Systolic and Diastolic Cardiac Function by CMR. J. Cardiovasc. Magn. Reson. 11(30) (2009)